<Original>

Extrusion of Viscoplastic Material

Hung Kuk Oh*

(Received September 25, 1980)

점소성 재료의 압출

오 홍 국

초 록

1200°C—1300°C의 열간 단조 작업에서의 강철은 스트레인 속도에 민감하고 그 기계적인 특성방정식은 $\bar{\sigma}=\sigma_0\dot{\bar{\varepsilon}}^m$ 이다. 이 연구는 열간압출시 필요로 하는 작용력을, 상계이론을 사용하여 해석하고 재료의 기계적 특성 상수들을 대입하여, 계산한다. 이 결과를 실험치와 비교하고 압출각, 마찰계수, 스트레인 속도와 점성계수등의 일반적인 영향에 대해서도 토의하였다.

특히 변형역내의 평균스트레인 속도에 의한 일정 항복응력을 사용하였을 경우에 대해서도 비교 검토 되었다.

Nomenclature

$\bar{\sigma}$; Effective yield stress.
σ_0; Effective yield stress atunit strain rate
$\dot{\bar{\varepsilon}}$; Effective strain rate
m; Viscosity coefficient
τ; Shear stress
$\bar{m}$; Friction factor
R_0; Radius of an initial billet
R_f; Radius of an extruded billet
v_0; Entering materialvelocity
v_f; Leaving material velocity
α; Semi-cone angle of an extrusion die
r, θ, ϕ; Spherical coordinate system
r_0, r_f; Radii at entrance and exit in sperical coordinates, respecuively
U_i; Material velocity components
$\Gamma_1, \Gamma_2, \Gamma_3, \Gamma_4$; Discontinuity surfaces
$\dot{\varepsilon}_{ij}$; Strain rate components
$\dot{W}_i$; Internal energy rate of deformation
$\dot{W}_s$; Dissipated energy rate by shear
Δv; Velocity discontinuity
V; Volume of flow-field
$\dot{W}_t$; Total energy rate
σ_N; Normal pressure
L; Land length
D_0, D_f; Diameters at entrance and exit, respectively

* Member, Ajou University

1. Introduction

Avitzur(1) had analyzed by the upper bound method the axisymmetric extrusion of ideal material (obeying Mises yield law) which is not strain-hardening and neglects elastic deformation. The steels of hot forging at 1200°C—1300°C are viscous following the law;

$$\bar{\sigma}=\sigma_0\dot{\bar{\varepsilon}}^m \tag{1}$$

Rossard(2) using hot torsion test found

that the viscosity coefficient is 0.14—0.24 at the hot working temperature range for the usual chemical components of the forging steels. Using an upper bound solution the necessary working pressure for the process is calculated with an assumed flow-field which is similar to the real one. In order to simplify the calculation the following assumptions have been made; (i) The extrusion die is considered as rigid (without deformation) (ii) Strain-hardening and elastic deformation are neglected (iii) Friction is taken as $\tau=\bar{m}\frac{\bar{\sigma}}{\sqrt{3}}$. The influences of viscosity, die angle, reduction of area are examined. The difference of the working pressure between the analysis by eq. (1) and that by constant effective stress at an averaged strain rate in the deformed volume is determined. An experimental study was conducted and compared with analytical prediction.

2. Analysis

A kinematically admissible flow field is proposed (Fig. 1 and Fig. 2). There are 3 zones in which the flow-field is continuous. In the zones I and III material flow velocity is uniform and has an axial component only. By the volume constancy,

$$v_0=v_f(R_f/R_0)^2 \quad (2)$$

Deformation has not started in zone I

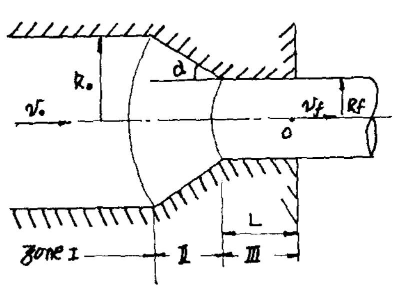

Fig. 1 Geometry of the process.

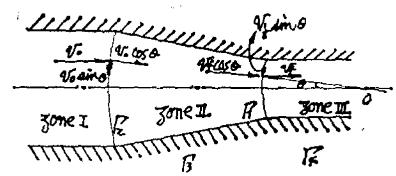

Fig. 2 Assumed flow-field.

which is seperated by Γ_2 from zone II. The surfaces Γ_2 and Γ_3 are assumed to be spherical and concentric with radius r_0 and r_f fron the apex O in spherical coordinates.

The velocity components are;

$$U_r=v=-v_f r_f^2\cos\theta/r^2,\ U_\theta=U_\phi=0 \quad (3)$$

There are tangential velocity discontinuities at the surfaces and;

$$\text{On the surfaces } \Gamma_1,\ \Delta v=v_f\sin\theta \quad (4)$$

$$\text{On the surface } \Gamma_2,\ \Delta v=v_0\sin\theta \quad (5)$$

The velocity discontinuities on the surfaces Γ_3, Γ_4 are;

$$\text{On the surface } \Gamma_3,\ \Delta v=v_f r_f^2\cos\alpha/r^2 \quad (6)$$

$$\text{On the surface } \Gamma_4,\ \Delta v=v_f \quad (7)$$

The internal energy of deformation and the dissipated energies at the discontinuity surfaces are calculated. The normalized working pressure is calculated from the total energy (see Appendix) as;

$$\frac{\sigma_N}{\sigma_0}=2^m\sin^m\alpha\left(\frac{v_f}{R_f}\right)^m\left\{\left(1-\frac{11}{12}\sin^2\alpha\right)^{\frac{m}{2}}+1\right\}\cdot\left\{\frac{2}{3m}\left(1-\frac{R_f^{3m}}{R_0^{3m}}\right)f(\alpha)+\frac{\alpha-\sin\alpha\cos\alpha}{2\sqrt{3}\sin^2\alpha}\left(1+\frac{R_f^{3m}}{R_0^{3m}}\right)\right\}+\frac{2\bar{m}}{3^{\frac{m+1}{2}}}(12\cos^2\alpha+\sin^2\alpha)^{m/2}\left(\frac{v_f}{R_f}\right)^m\sin^m\alpha\cdot\left\{\frac{\cos\alpha}{3m\sin\alpha}\left(1-\frac{R_f^{3m}}{R_0^{3m}}\right)+\frac{L}{R_f}\right\} \quad (8)$$

The influences of the die angle α and the reduction of area are shown in Fig. 3 and Fig. 4 where the normal pressure increases with α and reduction of area which is similar to the case for an ideal material. The influence of viscosity is shown in Fig. 5.

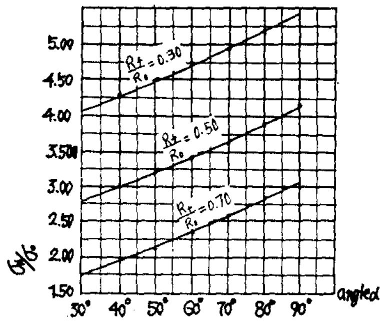

Fig. 3 Variation of working pressure with respect to die angle.

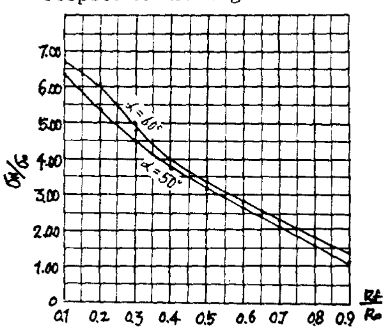

Fig. 4 Variation of normalized working pressure with respect to Rf/Ro.
* Reduction of area$=1-(Ro/Rf)^2$

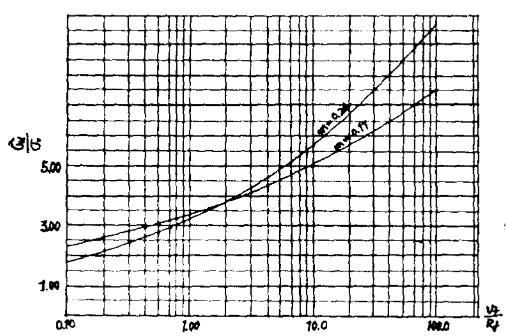

Fig. 5 Variation of normalized working pressure with respect to v_f/R_f.
* A is the point at which the average strain rate in the deformed volume is $1\ sec^{-1}$.

When the average strain rate in the deformed volume $(=3\frac{v_f}{R_0}\cdot\frac{(R_f/R_0)^2}{R_0\{1-(R_f/R_0)^2\}(1-\cos\alpha)}\ln\frac{R_0}{R_f}f(\alpha)\ \sin^2\alpha)$ is greater than $1\ sec^{-1}$, the normalized pressure increases with the viscosity coefficient (m).

3. Experiment

Twelve specimens were extruded using a 400 ton press. Six were extruded at a 76.6% reduction of area (D_0 : 62mm D_f : 30mm) and six at a 62.4% reduction of area (D_0 : 62mm D_f : 38mm). Before each operation, the specimens were preheated 20 minutes at 650°C and then 20 minutes at 850°C. Glass powder was used as a lubricant which has a friction coefficient of $\bar{m}=0.10$. This was determined by a ring test at hot forging conditions (7). The test material (38C2 in French standard specification) of 0.38% C and 0.2% Cr has been analyzed by Rossard (see Ref. 2) using a hot torsion test (Table 1). Extrusion forces and velocities were measured by load cell and a Displacement Transducer (Table 2, Table 3)

Table 1 Characteristics of the material.
Material; 38C2

Temperature	900°C	1000°C	1100°C	1200°C
σ_0(kg/mm²sec^m)	16.1	11.3	8.7	5.9
m	0.12	0.14	0.18	0.20

Table 2 Measured forces and velocities in case of 76.6% reduction of area.

Temperature	1100°C	1200°C	1300°C
Force (tons)	154.5	138.5	90.5
Velocity(mm/sec)	360	380	380

Table 3 Measured forces and velocities in case of 62.4% reduction of area.

Temperature	1100°C	1200°C	1300°C
Force (tons)	122.5	93.2	74.6
Velocity mm/sec	370	380	386

4. Results

(a) Comparison between analytical results and experiment. Because the friction between container wall and slug was not considered in the analysis, the forces were measured at the end of the steady state condition of the extrusion. The influence of deforming velocity on friction between the deforming zone and the die wall were assumed to be, $\tau=\bar{m}\frac{\bar{\sigma}}{\sqrt{3}}$, since the effective stress is a function of deformingvelocity (eq. (A14)). The required analytical forces were calculated for each reduction of area using experimental data and material characteristics from ROSSARD(2) at two temperatures (1100°C and 1200°C) (Table 1). There was very good agreement between analytical and experimental results except for one case (1100°C, 62.4% reduction of area) as shown in Table 4.

Table 4 Comparison between analytical force and experimental one.

Temperature	1100°C		1200°C	
R_f/R_0	0.6129	0.4839	0.6129	0.4839
v_f/R_f (sec^{-1})	25.9	51.3	26.6	54.1
$\bar{m}$	0.10	0.10	0.10	0.10
m	0.18	0.18	0.20	0.20
α	55°	65°	55°	65°
$f(\alpha)$	1.02677	1.04384	1.02677	1.04384
L/R_f	0.0	0.0	0.0	0.0
σ_N/σ_0	4.7918	7.2816	5.0986	7.8500
Force (tons)	125	191	91	139
Test force (tons)	123	155	93	139

(b) Comparison between classical method and eq. (8)

Normalized pressures were also calculated for one for an ideal material and the other using the averaged effective yield stress for a viscous material in the deforming volume. About 10% difference between the latter and eq. (8) was found at each test condition. as shown in Table 5 Therefore the velocity distribution effect in the deforming zone can not be neglected.

Table 5 Comparison between classical method and eq. (8)

Temperature	1100°C		1200°C	
R_f/R_0	0.6129	0.4839	0.6129	0.4839
α	55°	65°	55°	65°
A;/by eq.(8)	4.79	7.28	5.10	7.85
R_f/R_0	0.6129	0.4839	0.6129	0.4839
α	55°	65°	55°	65°
B; σ_N/σ_0 for an ideal material	2.09	4.13	2.09	4.13
C; σ_N/σ_0 for $\bar{\sigma}=\sigma_0\dot{\bar{\varepsilon}}^m$ average	5.03	7.87	5.71	8.55
D; % of difference between A and C	11%	8%	12%	9%

5. Conclusion

(i) The chracteristics of viscoplastic model, $\bar{\sigma}=\sigma_0\dot{\bar{\varepsilon}}^m$, are well adapted to hot extrusion.

(ii) The deformation rate of each point in the deforming zone must be considered. The averaged effective yield stress is less preferable.

(iii) The normalized pressure increases with α, $\bar{m}$ and L as in the case of ideal material.

(iv) The normalized pressure increases with m at $\dot{\bar{\varepsilon}}$ average >1 sec^{-1} and decreases at $\dot{\bar{\varepsilon}}$ average <1 sec^{-1}

Appendix

A. Analysis by upper bound

In the zone III, $R=r_f\sin\theta$, $dR=r_f\cos\theta d\theta$

$$\dot{V}=2\pi R dR v_f=2\pi v_f r_f^2\sin\theta\cos\theta d\theta \quad \text{(A1)}$$

In the zone II, $\dot{V}=-2\pi r\sin\theta r d\theta U_r$ (A2)

From eq. (A1) and eq. (A2)

$$U_r=-v_f r_f^2\cos\theta/r^2 \quad \text{(A3)}$$

(a) Internal energy of deformation ($\dot{W}_i$)

At the zone II, there is the symmtry of ϕ axis.

$$\varepsilon_{rr}=\frac{\partial U_r}{\partial r},\ \varepsilon_{\theta\theta}=U_r/r,\ \varepsilon_{\phi\phi}=U_r/r=-(\varepsilon_{rr}+\varepsilon_{\theta\theta})$$

$$\varepsilon_{r\theta}=\frac{1}{2r}\frac{\partial U_r}{\partial\theta},\quad \varepsilon_{\theta\phi}=\varepsilon_{r\phi}=0 \qquad \text{(A4)}$$

Applying eq. (3) into eq. (A4)

$$\varepsilon_{rr}=-2\varepsilon_{\theta\theta}=-2\varepsilon_{\phi\phi}=2v_f r_f^2\cos\theta/r^3$$

$$\varepsilon_{r\theta}=\frac{1}{2}v_f r_f^2\sin\theta/r^3,\quad \varepsilon_{\theta\phi}=\varepsilon_{r\phi}=0 \qquad \text{(A5)}$$

And then the effective strain rate;

$$\dot{\varepsilon}=\frac{\sqrt{2}}{\sqrt{3}}(\varepsilon_{rr}^2+\varepsilon_{\theta\theta}^2+\varepsilon_{\phi\phi}^2+2\varepsilon_{\theta\phi}^2)^{1/2}$$

$$=\frac{v_f}{\sqrt{3}}\frac{r_f^2}{r^3}(12\cos^3\theta+\sin^2\theta)^{1/2} \qquad \text{(A6)}$$

The internal energy $\dot{W}_i=\int_V \sigma\dot{\varepsilon}dV$

$$=\int_V \sigma_0\dot{\varepsilon}^{m+1}dV$$

where $dV=2\pi r\sin\theta rd\theta dr$

$$\dot{W}_i=\frac{2^{m+1}}{3m}\sigma_0\pi v_f^{1+m}\left[\frac{R_f^2}{R_f^m}-\frac{R_f^{2m+2}}{R_0^{3m}}\right]$$

$$\sin^m\alpha\cdot\left\{(1-\frac{11}{12}\sin^2\alpha)^{m/2}+1\right\}\cdot f(\alpha) \qquad \text{(A7)}$$

$$\text{where } f(\alpha)=\frac{1}{\sin^2\alpha}\left[1-\cos\alpha\sqrt{1-\frac{11}{12}\sin^2\alpha}+\frac{1}{\sqrt{11\cdot 12}}\ln\frac{1+\sqrt{\frac{11}{12}}}{\sqrt{\frac{11}{12}}\cos\alpha+\sqrt{1-\frac{11}{12}\sin^2\alpha}}\right]$$

(b) Dissipated energy at the discontinuity surfaces

$$\dot{W}_{s1,2}=\int_{\Gamma 1}\tau\Delta v dA+\int_{\Gamma 2}\tau\Delta v dA \qquad \text{(A8)}$$

$$\text{where } \tau=\frac{\sigma_0}{\sqrt{3}}\dot{\varepsilon}^m=\frac{\sigma_0}{\sqrt{3}}\frac{v_f^m}{(\sqrt{3})^m}\frac{r_f^{2m}}{r^{3m}}$$

$$(12\cos^2\theta+\sin^2\theta)^{m/2} \qquad \text{(A9)}$$

$$dA=2\pi r_f^2\sin\theta d\theta \qquad \text{(A10)}$$

$$\dot{W}_{s1,2}=\frac{1}{4}\left\{(1-\frac{11}{12}\sin^2\alpha)^{m/2}+1\right\}(\alpha-\sin\alpha\cos\alpha)$$

$$\frac{2^{1+m}}{\sqrt{3}}\pi\sigma_0 v_f^{1+m}r_f^{2-m}\left\{1+\left(\frac{r_f}{r_0}\right)^{3m}\right\} \qquad \text{(A11)}$$

And then $\dot{W}_{s3}=\int_{\Gamma 3}\tau\Delta v ds$ (A12)

where $ds=2\pi(dR/\sin\alpha)R$ (A13)

$$\tau=\frac{\bar{m}\sigma_0}{3^{(m+1)/2}}v_f^m\frac{R_f^{2m}}{R^{3m}}\sin^m\alpha$$

$$(12\cos^2\alpha+\sin^2\alpha)^{m/2} \qquad \text{(A14)}$$

$$\dot{W}_{s3}=\frac{2\pi\bar{m}\sigma_0}{3m3^{(1+m)/2}}v_f^{1+m}\sin^{m-1}\alpha\cos\alpha(12\cos^2\alpha$$

$$+\sin^2\alpha)^{m/2}R_f^{2m+2}\left(\frac{1}{R_f^{3m}}-\frac{1}{R_0^{3m}}\right) \qquad \text{(A15)}$$

And also $\dot{W}_{s4}=\int_{\Gamma 4}\tau\Delta v ds$ (A16)

$$\text{where } \tau=\frac{\bar{m}}{\sqrt{3}}\sigma_0\frac{v_f^m}{\sqrt{3}\cdot m\cdot\pi_f^m}(12\cos^2\alpha$$

$$+\sin^2\alpha)^{m/2} \qquad \text{(A17)}$$

$$\dot{W}_{s4}=\frac{2\pi\bar{m}\sigma_0}{3^{(m+1)/2}}v_f^{1+m}R_f^{1-m}\sin^m\alpha(12\cos^2\alpha$$

$$+\sin^2\alpha)^{m/2}\cdot L \qquad \text{(A18)}$$

(c) Total energy and normalized extrusion pressure

$$\dot{W}_t=\dot{W}_i+\dot{W}_{s1,2}+\dot{W}_{s3}+\dot{W}_{s4} \qquad \text{(A19)}$$

$$\frac{\sigma_N}{\sigma_0}=\dot{W}_t/\pi R_0^2\sigma_0 v_0 \qquad \text{(A20)}$$

References

1. Betzalel Avitzur, "Metal forming Process and analysis", McGrawHill, page 153-217, 1979
2. Rossard C., "Recrystallisation sous l'effect de la déformation plastique dans le façonnage à chaud", 7ème colloque de métallurgie, Saclay, 1963, page 112-123
3. Hoffmanner A.L., "Metal forming", Plenum press, New York, London, 1971, "The extrusion of rate sensitive materials", page 115-129
4. Kudo H., "Some analytical and experimental studies of axisymmetric cold forming and extrusion", part 1 and part 2, International Journal of Mech. Sci., Vol. 2, page 102-107, Vol. 3, page 91-117, 1961
5. De Lepinau E., Baque P., "Filage à chaud non-lubrifié", Rapport 028, 1973, Ecole des Mines de Paris
6. Thèse de Doc. Ing. Paris 6, "Sur le forgeage à chaud (simulation par plasticine)", page 92-113, Oh Hung Kuk, 1980
7. Ibid, page 33-47